Linking hopping conductivity to giant dielectric permittivity in oxides

A. Artemenko,[1,2,a)] C. Elissalde,[2] U.-C. Chung,[2] C. Estournès,[3] S. Mornet,[2] I. Bykov,[1] and M. Maglione[2]
[1]*Institute for Problems of Material Science, NASc of Ukraine, 3 Krjijanovskogo Street, 03680 Kiev-142, Ukraine*
[2]*ICMCB-CNRS, Université Bordeaux, F-33608 Pessac Cedex, France*
[3]*CIRIMAT et Plateforme Nationale CNRS de Frittage Flash, PNF2-CNRS, MHT, Université Paul Sabatier, 33062 Toulouse, France*

With the promise of electronics breakthrough, giant dielectric permittivity materials are under deep investigations. In most of the oxides where such behavior was observed, charged defects at interfaces are quoted for such giant behavior to occur but the underlying conduction and localization mechanisms are not well known. Comparing macroscopic dielectric relaxation to microscopic dynamics of charged defects resulting from electron paramagnetic resonance investigations we identify the actual charged defects in the case of $BaTiO_3$ ceramics and composites. This link between the thermal activation at these two complementary scales may be extended to the numerous oxides were giant dielectric behavior was found.

To overcome the well established dielectric permittivity of ferroelectric materials ($\varepsilon \sim 10^4$), a quest for so called giant permittivity compounds ($\varepsilon \sim 10^5$) has started from the beginning of the 2000s. In classical ferroelectrics, the dielectric permittivity is strongly temperature dependent with a divergence at a critical temperature. Many oxides are now available that display very specific features which are at variance from this behavior. In $CaCu_3Ti_4O_{12}$,[1,2] doped NiO,[3] $LuFe_2O_4$,[4] substituted $BaTiO_3$,[5] unprecedented ($\varepsilon \sim 10^5$) permittivity is observed which is temperature independent in the vicinity of room temperature before falling off below 200 K. This sharp decrease of ε going along with a strong maximum of the dielectric losses tan (δ) follows a single time dielectric relaxation. This relaxation time obeys an Arrhenius law with thermal activation energy around 0.1–0.4 eV for all the oxides listed above. Such common features in very different chemical compounds call for a model of broad use. The interface barrier layer ceramics (IBLC) drawn for $CaCu_3Ti_4O_{12}$ (Ref. 6) can be applied to all the materials listed above and many others. The major trends in this picture are that both geometrical confinement and charge accumulation at interfaces increase artificially the apparent dielectric permittivity. This is very similar to what is used every day in the mass production of supercapacitors.[7]

The IBLC model can be applied to any material where extended dielectric interfaces of very small thickness split (semi-)conducting parts:[8] in ceramics, insulating grain boundaries are surrounding conducting grains;[6] in thin films and multilayers, surfaces and intergrowth planes can induce dielectric barrier between conducting layers;[9,10] in single crystals, surfaces, two-dimensional (2D) defects like twin boundaries and structural domain walls can act as a dielectric barrier. However, the exact nature of the conduction mechanism within the grains and of the charge accumulation at the grain boundaries is not well understood. This motivated us to find a model system and relevant experiments which could help investigating and controlling the IBLC parameters.

In previous studies we used core@shell concept (the initial $BaTiO_3$ core particles were covered, using a sol-gel method, by a highly insulating SiO_2 shell[11]) to fix the structure and chemistry of the grain boundary in the final dense ceramics. The advanced sintering processes allow keeping the continuous nanometer size silica shell (density >95% of the theoretical one)[12] and stabilizing a reduced state of $BaTiO_3$ (BT) making it semiconducting without totally screening the intrinsic ferroelectric properties in the final ceramics.[13] We thus meet the two requirements of the IBLC model: (i) conducting grains separated by insulating grain boundaries and (ii) giant permittivity while keeping the underlying ferroelectric properties of BT. We also evidenced the dielectric relaxation with activation energy of 0.1 eV (Ref. 13) on which we focus in the present letter. We show the link between the macroscopic dielectric relaxation parameters and microscopic charged defects confirming that defect related conduction in reduced BT is the main ingredient for the giant permittivity. We also show that electron paramagnetic resonance (EPR) with the highest sensitivity to paramagnetic defects is the most suitable technique for probing such charged defects and we suggest its use when dealing with materials exhibiting giant permittivity.

Ceramic materials ($BaTiO_3$@SiO_2 and $BaTiO_3$) were prepared using spark plasma sintering (SPS) at 1200 °C under uniaxial pressure of 50 MPa in vacuum (for details see Ref. 12). After the sintering all samples have a dark blue color. A postannealing at 800 °C for 12 h in air is usually performed directly after SPS for removing carbon contamination of the samples, coming from the graphite die. In the case of BT ceramics such postannealing leads to the reoxidation of the sample which recovers white color. The silica shell prevents such reoxidation in the case of BT@Si composites and depending on silica shell thickness, the pellets remain of blue or dark blue color highlighting high concentration of defects (see Fig. 1).

The concentration of defects is important to obtain high permittivity value, but the dielectric barrier thickness has to

a)Electronic mail: alla.artemenko@live.co.uk.

[doi:10.1063/1.3495779]

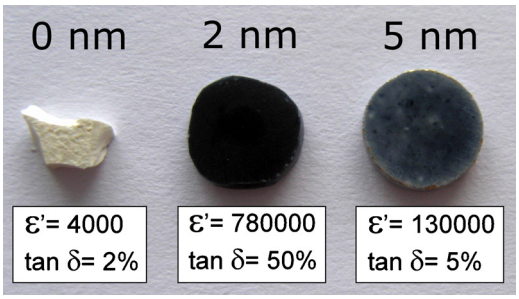

FIG. 1. (Color online) Photos and room temperature dielectric properties of SPS sintered and reoxidized BT@Si ceramics with different silica shell thickness: 0, 2, and 5 nm.

be optimized to minimize the losses and to keep ferroelectric properties of the BT core. The tunability of the dielectric permittivity and losses as a function of the silica shell thickness (which acts also as a dielectric barrier) is shown in Fig. 1. Increasing the silica shell up to 5 nm enables to sensibly decrease the 10 kHz dielectric losses while keeping giant permittivity (1.3×10^5) in an extended temperature range. However, the low temperature relaxation which occurs below 200 K leads to a strong increase of dielectric losses.[13]

Hereafter we will focus on the valence state of defects sensitive to annealing treatments and silica shell thickness to find out the link between these defects and the overall giant dielectric properties. Prominent signature of low temperatures EPR spectra of BT single crystals and thin films are ascribed to oxygen-deficient-related charged defects[14] or polaronic states of titanium.[15,16] These results are used for the interpretation of EPR spectra of BT@Si composite. We have performed proof-of-principle experiment on an example of current interest for EPR, the readout of charge defects valence states in BT and BT@Si ceramics. The EPR spectrum recorded at 4 K in a reoxidized BT500@Si5 ceramics (500 nm BT core and 5 nm silica shell) is shown in Fig. 2(a) (spectrum b). It differs from the BT500@Si2 analog only by small differences in the intensities and linewidths of some resonances. In addition to Fe^{3+} and Mn^{2+} impurities, the most intensive EPR resonances are located in the magnetic field region 3400–4000 G. To identify charged defects leading to these resonances, EPR temperature dependence studies were also performed on BT500@Si5 "green composite" (coated at room temperature before any thermal treatments), BT sintered using SPS before and after postannealing in oxygen atmosphere, and BT "green powder," correspondingly spectra (a, c, d, and e) in Fig. 2(a). They visually show that new charged defects are created during SPS sintering in both BT and BT@Si ceramics giving intensive EPRs. Postannealing leads to a full disappearance of these resonances for BT ceramics while they remain for BT@Si composite [see spectra b and d in Fig. 2(a)]. An exactly similar trend is observed with the color of the different samples which is white in BT and blue otherwise (Fig. 1). The color persistence in the composite is due to the fact that the silica shell prevents the reoxidation of the oxygen-deficiency-related defects created during SPS sintering thus maintaining semiconducting BT core.

We further focus only on the EPRs which are common to BT and BT@Si ceramic and that are affected by the annealing treatments. Keeping in mind that resonances originating from the same paramagnetic defects exhibit similar temperature behavior, we could separate the contribution arising from the different charged defects and unambiguously identify oxygen-deficiency-related defects in BT and BT@Si ceramics. As an example, Fig. 2(b) shows EPR spectra temperature dependence of BT500@Si5 ceramics. Two resonances at g=1.987 and g=1.945 are ascribed to Ti^{3+}-V(O) defect which represents a donor-type defect exhibiting an axial symmetry where oxygen vacancy is binding an electron located at a Ti^{3+} e_g ($3d^2_{3z}$-r^2) orbital. Negative shift in g-factor value from the one of the free electron, g-g_e, is indicating an electron-trapped-type origin of these defects. In addition, (i) both resonances are sensitive to the annealing treatments condition, confirming the presence of oxygen vacancy in nearest neighbor environment, (ii) the concentration of defects estimated from the EPR is of the order of 10^{18}–10^{20} cm^{-3}, being too high for unwanted impurities. This allows linking the oxygen-deficiency-related defects [Ti^{3+}-V(O)] to the samples color and hopping conductivity occurring between Ti ions.

The temperature dependence of Ti^{3+}-V(O) EPRs linewidth obeys an Arrhenius law [$\Delta B(T)=\Delta B_0 \exp(-E_a/kT)$] as shown in Fig. 3 (right scale). This agrees well with the dielectric relaxation activation law which is also shown in Fig. 3 (left scale) confirming that the electronic localization on Ti^{3+}-V(O) centers is connected with the interfacial relaxation leading to giant permittivity behavior. Within the IBLC model, we suggest that the Ti^{3+}-V(O) centers create an energy level close to the bottom of the BT conduction band which increase the grain conductivity through electronic hopping. Successive localization of such hopping electrons at the centers located close to grain boundaries lead to increased permittivity which relaxes with the same activation energy as the inner grain hopping conductivity, about 100 meV.

Additional electron trapping centers were also identified and they essentially confirm the barrier role of the silica shell

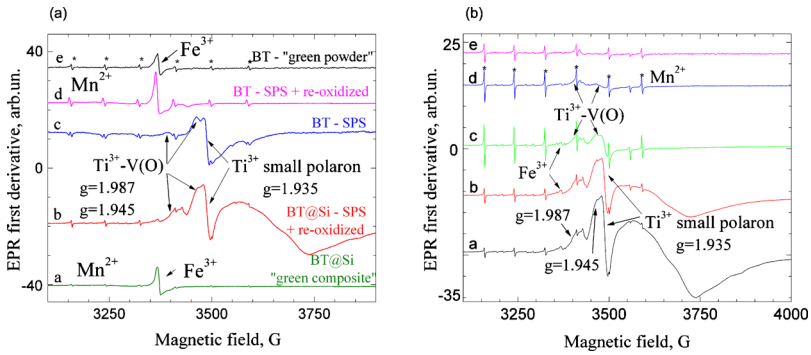

FIG. 2. (Color online) (a) EPR spectra recorded at 4 K in: a-BT500@Si5 "green composite," b-BT500@Si5 SPS sintered and reoxidized, c-BT ceramics SPS sintered, d-BT ceramics SPS sintered and reoxidized, e-BT "green powder" with particles size 500 nm; (b)-EPR spectra of SPS sintered and reoxidized BT500@Si5 composite recorded at several temperatures: a—4 K, b—20 K, c—50 K, d—60 K, and e—100 K (intensity multiplied by 2).

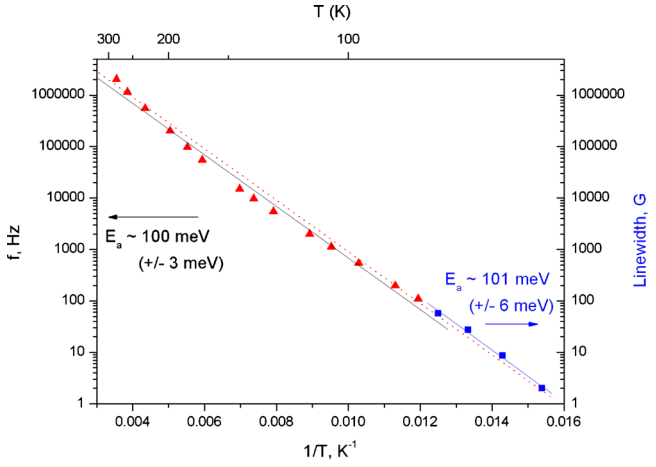

FIG. 3. (Color online) Dielectric relaxation time (left scale, taken from Ref. 13) and Ti^{3+}-V(O) linewidth vs temperature in an Arrhenius scale. The common slope (100 meV) of both lines calls for a common origin for these two mechanisms.

as already observed for Ti^{3+} related centers. For instance, the signal of Fe^{3+} fully disappears in the case of the SPS sintered BT as expected from its reduction to low spin Fe^{2+} (S=0), while it is still present in the SPS sintered coated samples [see spectra c and b in Fig. 2(a)]. This confirms the silica shell influence on the limited reoxidation of core-shell composites and hence on the valence state of intrinsic and impurity ions.

Another possible mechanism of electron localization in BT is the formation of polaronic type defects which also were observed in both BT and BT@Si ceramics, (see Fig. 2). Small polarons are very sensitive to the local stress indicating their location in vicinity of grain boundaries or composite interface. Broad intensive line observed only in BT@Si ceramics [spectrum b in Fig. 2(a)] in the magnetic field region 3500–3750 G can be attributed to defects located at composite interface. The discussion on the detailed model for such defects is out of the scope of the present paper and will require further investigations.

We propose that the unprecedented room temperature permittivity and strong maximum in the dielectric losses with thermal activation energy between 0.1–0.4 eV observed in some oxides, can be ascribed to the electron trapped at oxygen vacancy with further localization at one of host lattice cation, and accumulation at 2D defects such as grain boundaries in ceramics. In particular, in BT based ceramics, the hopping conductivity among Ti^{3+}-V(O) defects induces such space charges at internal barriers. The dynamics of these space charges is thus intimately related to the hopping mobility of electrons at Ti^{3+}-V(O) as shown from the similar activation energy for the dielectric relaxation and for the EPR linewidths. As a consequence, the giant dielectric behavior of $BaTiO_3$ based ceramics can be ascribed to electronic excitations. This is an important result for the anticipated use of these materials in supercapacitors. Indeed, all commercially available supercapacitors are based on ionic charges which accumulate at interfaces. Such ionic accumulation raises several issues such as slow dynamics and long term stability resulting from large lattice distortions. In this respect, electron-based supercapacitors may provide interesting opportunities.

To summarize, thanks to the combination of core-shell architecture and SPS we have demonstrated an efficient way to control and stabilize oxygen–deficiency-related defects in BT-based ceramics ($BaTiO_3$@SiO_2). EPR has allowed identifying charged defects responsible for both color change and extrinsic giant dielectric properties of reduced BT core. In addition, a close link between the macroscopic dielectric relaxation and the microscopic dynamics of charged defects was clearly evidenced: the value of activation energy of Ti^{3+}-V(O) centers calculated from EPR lies in the same range of that obtained from the dielectric measurements ($E_a \cong 0.1$ eV). Since this activation energy is similar in several different oxides[1–5] we suggest that shallow trap levels close to the bottom of the conduction band do occur in all these materials. Evidencing such defects through appropriate EPR investigations in these many materials would give a strong microscopic support to the internal barrier layer capacitor model.[6]

We acknowledge financial support from the European Community through the FAME Erasmus Mundus program, from the French National Agency for Research under Contract No. ANR NANO4F and from Ukrainian-French exchange program DNIPRO 19716PB. We also thank A. Villesuzanne and M. Pollet for valuable advice for the critical reading of article.

[1]A. P. Ramirez, M. A. Subramanian, M. Gardel, G. Blumberg, D. Li, T. Vogt, and S. M. Shapiro, Solid State Commun. **115**, 217 (2000).
[2]D. Capsoni, M. Bini, V. Massarotti, G. Chiodelli, M. C. Mozzatic, and C. B. Azzoni, J. Solid State Chem. **177**, 4494 (2004).
[3]J. Wu, C.-W. Nan, Y. Lin, and Y. Denget, Phys. Rev. Lett. **89**, 217601 (2002).
[4]N. Ikeda, H. Ohsumi, K. Ohwada, K. Ishii, T. Inami, K. Kakurai, Y. Murakami, K. Yoshii, S. Mori, Y. Horibe, and H. Kitô, Nature (London) **436**, 1136 (2005).
[5]I. P. Raevski, S. A. Prosandeev, A. S. Bogatin, M. A. Malitskaya, and L. Jastrabik, J. Appl. Phys. **93**, 4130 (2003).
[6]C. D. Sinclair, T. B. Adams, F. D. Morrison, and A. R. West, Appl. Phys. Lett. **80**, 2153 (2002).
[7]B. E. Conway, *Electrochemical Supercapacitors: Scientific Fundamentals and Technological Applications* (Springer, New York, 1999).
[8]M. Maglione, in *Springer Series of Topics in Solid-State Sciences*, edited by V. S. Vikhnin and G. K. Liu (Springer, New York, 2011).
[9]O. Trithaveesak, J. Schubert, and Ch. Buchal, J. Appl. Phys. **98**, 114101 (2005).
[10]L. Qiao and X. F. Bi, J. Phys. D: Appl. Phys. **42**, 175508 (2009).
[11]S. Mornet, C. Elissalde, O. Bidault, F. Weill, E. Sellier, O. Nguyen, and M. Maglione, Chem. Mater. **19**, 987 (2007).
[12]U.-C. Chung, C. Elissalde, F. Mompiou, J. Majimel, S. Gomez, C. Estournès, S. Marinel, A. Klein, F. Weill, D. Michau, S. Mornet, and M. Maglione, J. Am. Ceram. Soc. **93**, 865 (2010).
[13]U.-C. Chung, C. Elissalde, C. Estournès, and M. Maglione, Appl. Phys. Lett. **94**, 072903 (2009).
[14]V. V. Laguta, A. M. Slipenyuk, I. P. Bykov, M. D. Glinchuk, M. Maglione, D. Michau, J. Rosa, and L. Jastrabik, Appl. Phys. Lett. **87**, 022903 (2005).
[15]S. Lenjer, O. F. Schirmer, and H. Hesse, Phys. Rev. B **66**, 165106 (2002).
[16]V. V. Laguta, A. M. Slipenyuk, I. P. Bykov, M. D. Glinchuk, M. Maglione, A. G. Belous O. I. V'yunov, J. Rosa, and L. Jastrabik, J. Appl. Phys. **97**, 073707 (2005).